Nanostructures

DOI: 10.1002/anie.201007151

Alumina-Sheathed Nanocables with Cores Consisting of Various Structures and Materials**

Fangming Han, Guowen Meng, Qiaoling Xu, Xiaoguang Zhu, Xianglong Zhao, Bensong Chen, Xiangdong Li, Dachi Yang, Zhaoqin Chu, and Mingguang Kong*

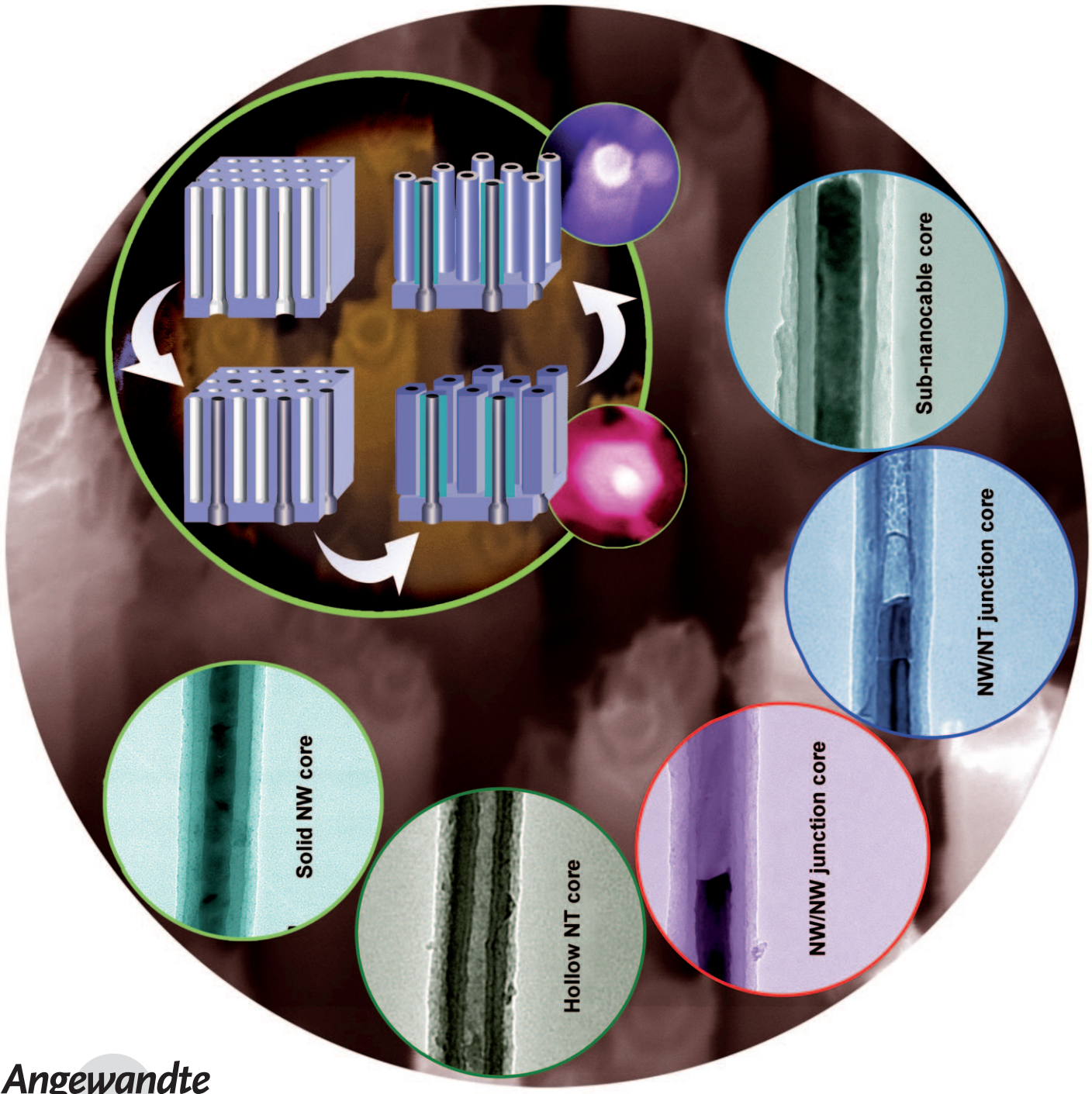

Nanocables have had a large impact on the development of nanotechnology.[1–4] Various nanocables with insulating outer sheaths of silica and alumina have been constructed;[5–16] these nanocables could be ideal components in nanoelectronics because the sheaths can act as protective layer, gate oxide, and dielectric.[2,10,15] However, present synthetic strategies have very limited control over the inner core materials and structures that are central to the rational design of nanoelectronics, nanosystems, and nanodevices. Herein we show a generic hard-template-based (using porous anodic aluminum oxide (AAO) with two-layer pores) synthetic approach for the precisely controlled fabrication of alumina-sheathed nanocables with various inner cores consisting of solid nanowire (NW), hollow nanotube (NT), axial NW/NW and NW/NT heterostructures, and core–shell structures of subnanocables with smaller diameters. This technique could have considerable implications in nanotechnology.

Nanoporous AAO has been studied for five decades.[17] Different pore morphologies and arrangements have been achieved under appropriate electrochemical conditions, and the AAO with these pore morphologies has been used as template for the synthesis of various 1D nanostructures. Hexagonally arranged straight cylindrical pores with the same diameter and length are usually produced by a simple two-step anodization under constant potential;[18] these pores have been widely used as template for the synthesis of NWs,[19] NTs,[20] and two-segment NW/NT[21,22] heterostructures with a linear topology. Branched pores could be created by reducing the anodizing voltage by a factor of $1/\sqrt{n}$ during the course of anodization,[23,24] and branched NWs, NTs, NW/NTs, and even three-segment NT/NW/NT hetero-nanostructures with a branched topology could be produced by using these pores as templates.[25] Masuda et al.[26] obtained ordered pores with a non-uniform barrier layer (the barrier layer was thinner at the un-imprinted sites than that at the imprinted sites) by anodizing Al substrate pre-imprinted by a SiC mold with an ordered array of convex dimples. The barrier layer at the un-imprinted sites was selectively penetrated by controlling the etching time of the barrier layer, and one metal was deposited in the penetrated pores; the barrier layer at the imprinted sites was then further penetrated, and a second metal was deposited, thus mosaic nanocomposites composed of gold and nickel NWs were formed in one piece of AAO template. Additionally, by using two consecutive processes of "mild" and "hard" anodization of the Al substrate, an ordered AAO template with high aspect ratios of uniform nanopores with modulated pore diameters[27,28] and a two-layer-pore "mild–hard" AAO template[29] were formed. Attention has also been paid to the synthesis of insulator-sheathed nanocables by an AAO template-assisted approach. For example, SiO_2-sheathed nanocables were produced by a combination of wet chemical template replication to form SiO_2 shells and a subsequent electrodeposition to form the cores.[9] Atomic layer deposition (ALD) was also used to fabricate core–shell nanocables inside the porous AAO template,[14–16] and the thickness of the shell could be precisely controlled by the number of ALD cycles, however, intricate ALD equipment has to be used. Meanwhile, simple etching from the planar surface of the AAO template embedded with NWs in the pores was also attempted for alumina-sheathed nanocables.[30] However, the resulting alumina-sheathed cables have a tapered morphology, as the etching occurs slowly from one planar surface to the other.

For a generic AAO template-assisted approach to alumina-sheathed nanocables, we purposely increased the anodizing voltage by a factor of $\sqrt{3}$ in the final anodization stage and maintained the increased voltage for a given period of time to obtain an AAO with a completely new structure (Figure 1 a). According to our previous work,[23] the number of the upper-layer pores is three times of that of the lower-layer pores, therefore after increasing the anodizing voltage for the last period of anodization, one-third of the pores continues to grow with a large diameter, while the remaining two-thirds of the pores stop growing (Figure 1 a, center). After removing the remaining Al and etching the bottom barrier layer (Figure 1 a, right), a two-layer-pore AAO template with a completely new-structure that consists of parallel two-end-through pores (denoted as through-pores) and top-through-bottom-capped pores (denoted as capped-pores), with each through-pore surrounded by six capped-pores in a hexagonal arrangement, was formed (Figure S1 in the Supporting Information). Figure 1 b shows an SEM image taken on the bottom cross-section of the AAO template. Figure 1 c, d shows the top view of the upper layer and the bottom view of lower layer. It can be seen that the distance of the next-nearest-neighbor pores of the upper layer is much closer to the interpore distance of bottom layer. (The detailed preparation process and structural analysis of the AAO template can be found in Figure S1 and the Experimental Details in the Supporting Information). By using the AAO as a template, we deposited various 1D (hetero-) nanostructures inside only the through-pores while leaving the capped-pores empty (Figure 1 e, left). We then filled the empty capped-pores with a wet chemical etching agent in order to selectively etch the walls between the capped-pores completely and further thin the walls of the through-pores (filled with cores) to form alumina-sheathed nanocables with both hexahedral (Figure 1 e, center) and columnar (Figure 1 e, right) sheaths by tuning the duration of the wet chemical etching. Theoretically, any 1D (hetero-) nanostructures that were previously synthesized by the AAO template-assisted approach could be built inside the through-pores to produce alumina-sheathed nano-

[*] Dr. F. M. Han, Prof. G. W. Meng, Dr. Q. L. Xu, X. G. Zhu, Dr. X. L. Zhao, Dr. B. S. Chen, Dr. X. D. Li, Dr. D. C. Yang, Z. Q. Chu, M. G. Kong
Key Laboratory of Materials Physics and
Anhui Key Laboratory of Nanomaterials and Nanostructures
Institute of Solid State Physics, Chinese Academy of Sciences
Hefei 230031 (People's Republic of China)
Fax: (+86) 551-559-1434
E-mail: gwmeng@issp.ac.cn

[**] This work was supported by the National Natural Science Foundation of China (grant nos. 50525207 and 50972145) and the National Basic Research Program of China (grant no. 2007CB936601). We also thank Xiaoli He for assistance with sample preparation.

Supporting information for this article is available on the WWW under http://dx.doi.org/10.1002/anie.201007151.

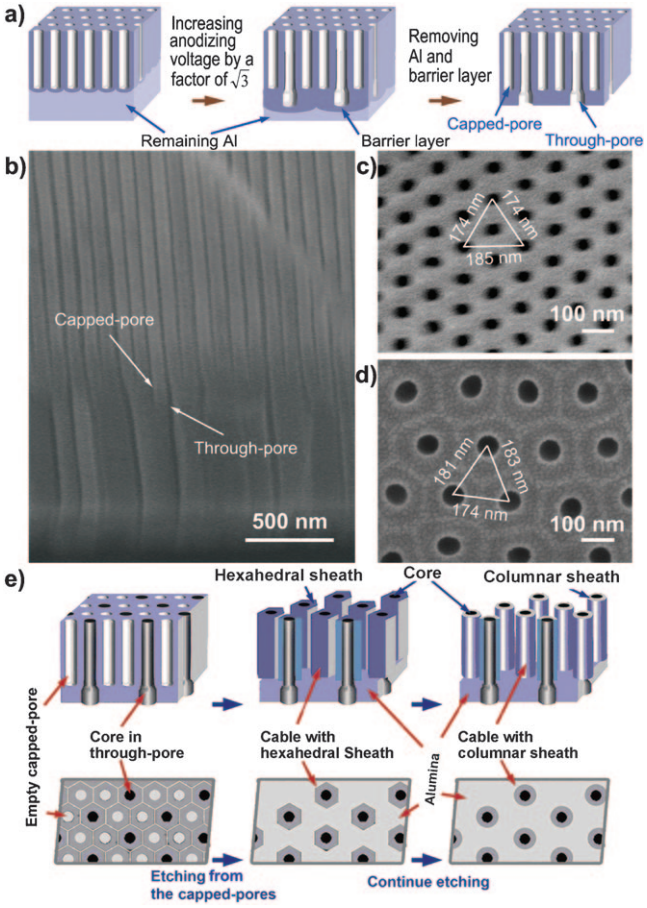

Figure 1. a) Preparation of the two-layer-pore AAO template. b) Side-view, c) top-view, and d) bottom-view SEM images of the two-layer-pore AAO template. e) Fabrication process of alumina-sheathed nanocables with different sheath morphologies and thicknesses.

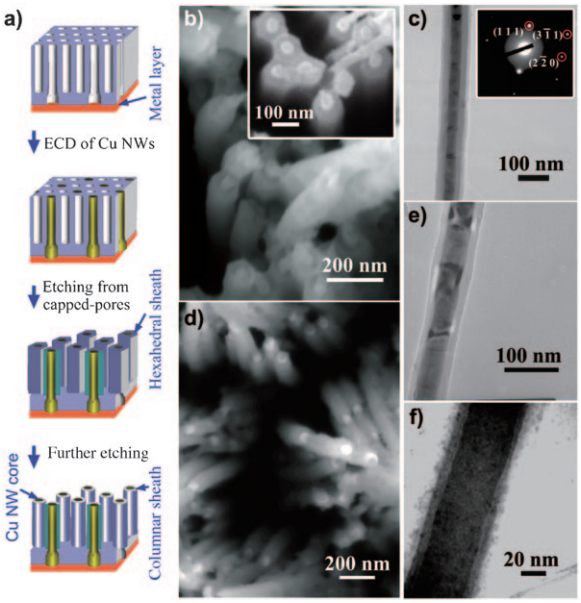

Figure 2. Alumina-sheathed nanocables with Cu NW cores. a) Fabrication process. b,c) Top-view SEM image and TEM image of the nanocables with hexahedral sheaths. The inset in (c) shows the SAED pattern. d,e) Top-view SEM and TEM images of the nanocables with columnar sheaths. f) Typical nanocable obtained by etching at 30 °C for 2 h.

cables with inner cores consisting of various materials and 1D (hetero-) nanoarchitectures.

Firstly, we tried to fill only the through-pores of the two-layer-pore AAO with solid NWs in order to produce alumina-sheathed nanocables with solid NWs as inner cores. Figure 2a shows the fabrication process, where a metal layer is sputtered onto the bottom planar surface side (with only through-pore openings) as working electrode (Figure S2a), and nanochannel-confined electrochemical deposition (ECD) is used to fill only the through-pores with solid NWs. Elemental metal NWs (e.g., Cu NWs) were electrodeposited inside only the through-pores of the two-layer-pore AAO template.[32] After wet chemical etching through the empty capped-pores in a 6% phosphoric acid solution at 30 °C, alumina-sheathed nanocables with solid Cu NWs as inner cores were formed (Figure 2b and Figure S2b). We further demonstrated that the morphology and thickness of the outer alumina sheath can be tailored by tuning the duration of the wet chemical etching; the diameters of the nanocables decrease linearly with the etching time (Figure S3). Usually, shorter etching times lead to hexahedral alumina sheaths with a large thickness (Figure 2b,c), while longer etching times lead to columnar alumina sheaths with a small thickness (Figure 2d,e), and much longer etching times lead to much thinner alumina sheaths (Figure 2f). The two apparent alumina shell layers in Figure 2c are actually projective shadows derived from the main body and the projecting areas of the hexagonal prism; the selected-area electron diffraction (SAED) pattern (inset) taken from the nanocable reveals the amorphous sheath and the single-crystalline nature of the solid Cu NW core, which is in agreement with our previous results.[32] Energy-dispersive X-ray (EDX) mapping (Figure S4) reveals that the nanocable consists of Cu, Al, and O, and the core–shell contrasts arise from the well-defined spatial distribution of elemental Cu in the core, and Al and O in the shell.

For the alumina-sheathed nanocables with solid NWs as inner cores produced by ECD, not only other metals (Zn NWs, Figure S5) and semimetals (Bi NWs, Figure S6), but also a wide range of other materials that are amenable to ECD can be created as solid NW cores of the alumina-sheathed nanocables. For example, the group II–VI compound semiconductor CdS and the conducting polymer polypyrrole (Figures S7 and S8) have been used as the solid NW inner cores in alumina-sheathed nanocables. Even semiconducting metal oxides of elemental metals that are amenable to ECD can be also constructed as solid NW inner cores. For example, alumina-sheathed nanocables with solid ZnO NWs as inner cores have been produced by a combinatorial process of ECD of pure metal Zn NW cores merely in the through-pores, converting the Zn NWs into ZnO NWs by simple oxidation,[19] and then selectively etching from the capped-pores (Figure S9).

We then tried to fill only the through-pores with hollow NTs in order to form alumina-sheathed nanocables with hollow NTs as cores. As carbon NTs (CNTs)[25] and silicon NTs (SiNTs)[33] could be formed inside the channels of the

AAO templates by AAO-self-catalyzed growth in chemical vapor deposition (CVD) processes, we then tried to fill CNTs and SiNTs inside only the through-pores of the two-layer-pore AAO templates to form alumina-sheathed nanocables with CNTs (Figure 3a) and SiNTs (Figure S10a) as cores, respectively. A dense silver layer was sputtered onto the planar surface of the smaller-diameter pore side of the two-layer-pore AAO template to prevent gaseous species from flowing into the capped-pores, while acetylene (C_2H_2) or silane (SiH_4) species can still enter only the through-pores from the template bottom to form CNTs[25] or SiNTs[33] by nanochannel-confined AAO-self-catalyzed growth. After removing the sputtered silver layer and selectively etching from the empty capped-pores, alumina-sheathed nanocables with CNTs (Figure 3) and SiNTs (Figure S10), respectively, were formed. As expected, etching for long periods leads to thin sheaths with a columniform shape (Figure 3b) and etching for short periods leads to thick sheaths with hexahedral cross-sections (Figure S11a). The enlarged image (inset in Figure 3b) shows the open tips of the CNTs. When the TEM observation (Figure 3c) and the EDX analysis (Figure S11b) are taken together, it can be seen that alumina-sheathed nanocables with CNTs as inner cores are formed. The high-resolution TEM (HRTEM) image of the nanocable (Figure 3d; taken from the area marked in red in Figure 3c) shows that the multiwalled CNTs are closely adhered to the alumina sheath. It should be noted that the alumina shells become polycrystalline after CVD growth of CNTs (Figure S11c,d), which would be important for the fabrication of functional devices by using the alumina-sheathed cables as building blocks. Additionally, as NTs of other materials that are amenable to ECD can be produced by ECD inside the channels of the AAO template coated with a thin meshlike Au layer as the electrode,[34] we coated a meshlike Au layer on the bottom large-pore-diameter side of the AAO template to grow NTs by ECD in only the through-pores. As expected, the alumina-sheathed nanocables with hollow NTs as inner cores (e.g., Ni NTs; Figure S12) were formed by further etching from the inside of the empty capped-pores.

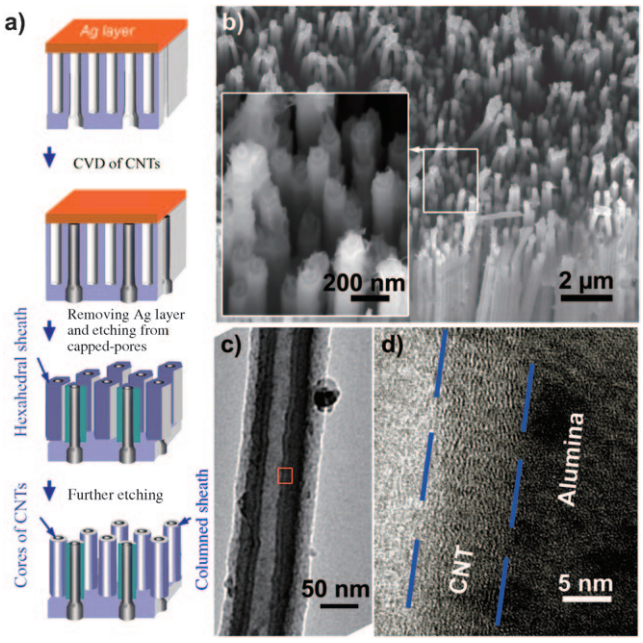

Figure 3. Alumina-sheathed nanocables with CNT cores. a) Fabrication process. b) SEM image of the nanocable arrays. The inset is the enlarged image taken from the white rectangle. c) TEM image of a single nanocable. d) HRTEM image of the nanocable. Dashed blue lines indicate the CNT wall.

We subsequently attempted to fill the through-pores with axial 1D hetero-nanostructures in order to produce alumina-sheathed nanocables with 1D hetero-nanostructures as cores. Firstly, sequential ECD of different materials in the through-pores was performed in order to obtain well-connected two-segment NWs as inner cores. For example, alumina-sheathed cables with axial 1D hetero-nanostructures of Au NWs and CdS NWs as cores were formed (Figure S13). Secondly, as the combination of sequential ECD and CVD can be used to build two-segment 1D hetero-nanostructures inside the pores of the AAO template,[21,24,25] we applied this technique in only the through-pores to obtain heterostructures of ECD-grown-NWs (e.g. Au NWs) and CVD-grown Ge NWs as cores (Figure S14). Thirdly, the inner cores of the alumina-sheathed nanocables can consist of not only two well-connected segments of solid NWs, but also axial heterostructures of solid NWs and hollow NTs. To illustrate this principle, we grew axial hetero-nanostructures of Cu NWs and CNTs inside only the through-pores by ECD of Cu NWs and subsequent CVD of CNTs, and then etched the metal layer and the walls between the capped-pores (Figure 4a). The TEM image of a typical nanocable (Figure 4b) reveals that the inner core consists of well-connected solid NWs and hollow NTs. The SAED pattern taken from the NWs segment (Figure 4b, inset) reveals the single-crystalline nature of the Cu NWs. The HRTEM image of the nanocable segment with CNT as core (Figure 4c) reveals that the multiwalled CNT is well adhered to the alumina sheath. The HRTEM image taken from the nanocable where the Cu NW and the CNT meet (Figure 4d) shows that the inner two segments of the Cu NW and CNT are indeed tightly connected with the end of the CNT close to the CuNW tip, as the tip acts as a cap during CVD growth of the CNTs.[24,25]

Finally, we tried to fill the through-pores with NTs and further fill the inner NTs with NWs to form alumina-sheathed nanocables with smaller-diameter sub-nanocables as cores. As materials that are amenable to ECD could be electrodeposited inside the AAO-grown CNTs to produce CNT-sheathed nanocables,[35] we firstly grew CNTs only inside the through-pores of the AAO template, then electrodeposited Cu_2O NWs[36] inside only these CVD-grown CNTs, and finally etched the metal electrode and the pore walls between the capped-pores. As a result, alumina-sheathed nanocables with smaller-diameter sub-nanocables of Cu_2O NW core/CNT sheath (CNT as the intermediate shell and Cu_2O NW as the inner core) were formed (Figure S15). As all these nanocables were produced by conventional ECD or high-temperature CVD, they are very stable.

In summary, we have created a two-layer-pore AAO template with parallel through-pores and capped-pores, where each through-pore is surrounded by six capped-pores in a hexagonal arrangement. By selectively filling 1D

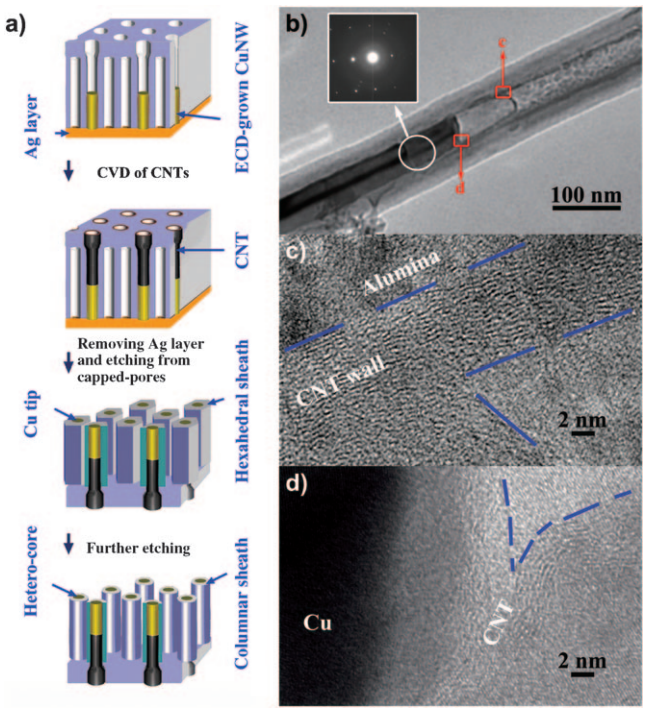

Figure 4. Alumina-sheathed nanocables with axial Cu NW/CNT heterostructure cores. a) Fabrication process. b) TEM image of a typical nanocable. The inset shows the SAED pattern taken from the region marked with white circle. c, d) HRTEM images of the nanocable taken from the two red rectangular areas marked in (b). Dashed blue lines indicate the CNT wall.

(hetero-) nanostructures in only the through-pores by ECD, electrochemical polymerization, CVD, and a combination of these methods, and subsequent wet chemical etching from the empty capped-pores, we have developed a powerful generic synthetic approach to a large variety of alumina-sheathed nanocables with inner cores that consist of solid NWs, hollow NTs, axial 1D heterostructures of NWs/NWs and NWs/NTs, and radial core–shell heterostructures of sub-nanocables with smaller diameters, where the inner NWs and NTs can be made from metals, metal oxides, compound semiconductors, conducting polymers, and elemental carbon, silicon, and germanium. This approach could have far-reaching implications in nanoscale electronics, devices, and systems, where alumina-sheathed nanocables with inner cores that consist of defined mono- and hetero-nanostructures and various materials are required.

Received: November 15, 2010
Published online: February 4, 2011

Keywords: aluminum oxide · anodization · etching · nanostructures · nanotubes

[1] L. J. Lauhon, M. S. Gudiksen, D. L. Wang, C. M. Lieber, *Nature* **2002**, *420*, 57–61.
[2] J. Xiang, W. Lu, Y. J. Hu, Y. Wu, H. Yan, C. M. Lieber, *Nature* **2006**, *441*, 489–493.
[3] J. Q. Hu, Q. Li, X. M. Meng, C. S. Lee, S. T. Lee, *Chem. Mater.* **2003**, *15*, 305–308.
[4] D. W. Kim, I. S. Hwang, S. J. Kwon, H. Y. Kang, K. S. Park, Y. J. Choi, K. J. Choi, J. G. Park, *Nano Lett.* **2007**, *7*, 3041–3045.
[5] Y. Zhang, K. Suenaga, C. Colliex, S. Iijima, *Science* **1998**, *281*, 973–975.
[6] H. Z. Zhang, X. H. Luo, J. Xu, B. Xiang, D. P. Yu, *J. Phys. Chem. B* **2004**, *108*, 14866–14869.
[7] J. H. He, Y. Y. Zhang, J. Liu, D. Moore, G. Bao, Z. L. Wang, *J. Phys. Chem. C* **2007**, *111*, 12152–12156.
[8] J. Hwang, B. Min, J. S. Lee, K. Keem, K. Cho, M. Y. Sung, M. S. Lee, S. Kim, *Adv. Mater.* **2004**, *16*, 422–425.
[9] N. I. Kovtyukhova, B. K. Kelley, T. E. Mallouk, *J. Am. Chem. Soc.* **2004**, *126*, 12738–12739.
[10] H. T. Ng, J. Han, T. Yamada, P. Nguyen, Y. P. Chen, M. Meyyappan, *Nano Lett.* **2004**, *4*, 1247–1252.
[11] L. Fu, Y. Q. Liu, Z. M. Liu, B. X. Han, L. C. Cao, D. C. Wei, G. Yu, D. B. Zhu, *Adv. Mater.* **2006**, *18*, 181–185.
[12] L. Zhang, R. Tu, H. J. Dai, *Nano Lett.* **2006**, *6*, 2785–2789.
[13] J. Y. Huang, S. Liu, Y. Wang, Z. Z. Ye, *Appl. Surf. Sci.* **2008**, *254*, 5917–5920.
[14] L. K. Tan, M. A. S. Chong, H. Gao, *J. Phys. Chem. C* **2008**, *112*, 69–73.
[15] J. M. Lee, S. Farhangfar, R. B. Yang, R. Scholz, M. Alexe, U. Gösele, J. Lee, K. Nielsch, *J. Mater. Chem.* **2009**, *19*, 7050–7054.
[16] Y. T. Chong, D. Görlitz, S. Martens, M. Y. E. Yau, S. Allende, J. Bachmann, K. Nielsch, *Adv. Mater.* **2010**, *22*, 2435–2439.
[17] F. Keller, M. S. Hunter, D. L. Robinson, *J. Electrochem. Soc.* **1953**, *100*, 411–419.
[18] H. Masuda, K. Fukuda, *Science* **1995**, *268*, 1466–1468.
[19] Y. Li, G. W. Meng, L. D. Zhang, F. Phillipp, *Appl. Phys. Lett.* **2000**, *76*, 2011–2013.
[20] W. Lee, R. Scholz, K. Nielsch, U. Gösele, *Angew. Chem.* **2005**, *117*, 6204–6208; *Angew. Chem. Int. Ed.* **2005**, *44*, 6050–6054.
[21] J. Luo, L. Zhang, Y. J. Zhang, J. Zhu, *Adv. Mater.* **2002**, *14*, 1413–1414.
[22] F. M. Han, G. W. Meng, X. L. Zhao, Q. L. Xu, J. X. Liu, B. S. Chen, X. G. Zhu, M. G. Kong, *Mater. Lett.* **2009**, *63*, 2249–2252.
[23] J. Li, C. Papadopoulos, J. Xu, *Nature* **1999**, *402*, 253–254.
[24] G. W. Meng, Y. J. Jung, A. Cao, R. Vajtai, P. M. Ajayan, *Proc. Natl. Acad. Sci. USA* **2005**, *102*, 7074–7078.
[25] G. W. Meng, F. M. Han, X. L. Zhao, B. S. Chen, D. C. Yang, J. X. Liu, Q. L. Xu, M. G. Kong, X. G. Zhu, Y. J. Jung, Y. J. Yang, Z. Q. Chu, M. Ye, S. Kar, R. Vajtai, P. M. Ajayan, *Angew. Chem.* **2009**, *121*, 7302–7306; *Angew. Chem. Int. Ed.* **2009**, *48*, 7166–7170.
[26] H. Masuda, A. Abe, M. Nakao, A. Yokoo, T. Tamamura, K. Nishio, *Adv. Mater.* **2003**, *15*, 161–164.
[27] W. Lee, R. Ji, U. Gösele, K. Nielsch, *Nat. Mater.* **2006**, *5*, 741–747.
[28] K. Schwirn, W. Lee, Reinald Hillebrand, M. Steinhart, K. Nielsch, U. Gösele, *ACS Nano* **2008**, *2*, 302–310.
[29] J. H. Lim, W. S. Chae, H. O. Lee, L. Malkinski, S. G. Min, J. B. Wiley, J. H. Jun, S. H. Lee, J. S. Jung, *J. Appl. Phys.* **2010**, *107*, 09A334.
[30] Y. W. Yang, L. Li, X. H. Huang, M. Ye, Y. C. Wu, G. H. Li, *Mater. Lett.* **2006**, *60*, 569–571.
[31] A. P. Li, F. Müller, A. Birner, K. Nielsch, U. Gösele, *J. Appl. Phys.* **1998**, *84*, 6023–6026.
[32] D. C. Yang, G. W. Meng, S. Y. Zhang, Y. F. Hao, X. H. An, Q. Wei, M. Ye, L. D. Zhang, *Chem. Commun.* **2007**, 1733–1735.
[33] B. S. Chen, G. W. Meng, Q. L. Xu, X. G. Zhu, M. G. Kong, Z. Q. Chu, F. M. Han, Z. Zhang, *ACS Nano* **2010**, *4*, 7105–7112 .
[34] D. C. Yang, G. W. Meng, Q. L. Xu, F. M. Han, M. G. Kong, L. D. Zhang, *J. Phys. Chem. C* **2008**, *112*, 8614–8616.
[35] C. Mu, Y. X. Yu, R. M. Wang, K. Wu, D. S. Xu, G. L. Guo, *Adv. Mater.* **2004**, *16*, 1550–1553.
[36] X. M. Liu, Y. C. Zhou, *Appl. Phys. A* **2005**, *81*, 685–689.